Langmuir

Subscriber access provided by KOOK MIN UNIV

Research Article

Effect of Layer Integrity of Spin Self-Assembled Multilayer Films on Surface Wettability

Jinhan Cho, and Kookheon Char

Langmuir, **2004**, 20 (10), 4011-4016 • DOI: 10.1021/la035476l

Downloaded from http://pubs.acs.org on December 30, 2008

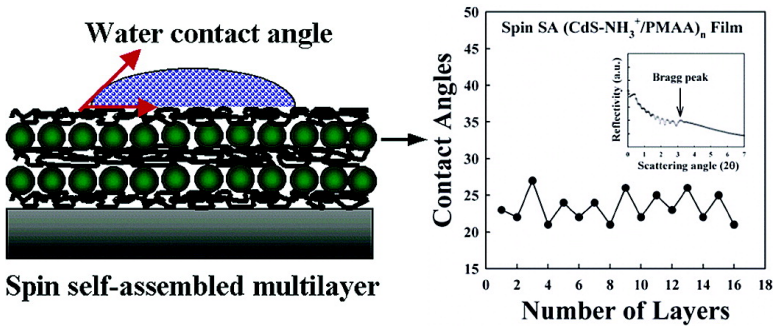

More About This Article

Additional resources and features associated with this article are available within the HTML version:

- Supporting Information
- Links to the 4 articles that cite this article, as of the time of this article download
- Access to high resolution figures
- Links to articles and content related to this article
- Copyright permission to reproduce figures and/or text from this article

View the Full Text HTML

ACS Publications
High quality. High impact.

Langmuir is published by the American Chemical Society. 1155 Sixteenth Street N.W., Washington, DC 20036

Effect of Layer Integrity of Spin Self-Assembled Multilayer Films on Surface Wettability

Jinhan Cho and Kookheon Char*

School of Chemical Engineering and Institute of Chemical Processes, Seoul National University, San 56-1, Shillim-dong, Kwanak-gu, Seoul 151-744, Korea

Received August 12, 2003. In Final Form: February 1, 2004

We investigated the correlation between surface wettability and internal structure of polyelectrolyte (PE)/PE and PE/inorganic multilayer films prepared by the spin self-assembly (SA) method. Spin self-assembled poly(allylamine hydrochloride) (PAH)/poly(sodium 4-styrenesulfonate) (PSS) multilayer films deposited from PE solutions of 10 mM show the distinct oscillation in contact angles with variation of the outermost PE layer, representing the saturated values in contact angles of individual PAH and PSS layers. These contact angles are also well consistent with the angles measured from respective PE layers (i.e., PAH and PSS) of the spin SA (PAH/CdS−COO^-) and (CdS−NH_3^+/PSS) films carrying the flat interface between PE and inorganic CdS nanoparticle layers as confirmed by X-ray reflectivity. Furthermore, based on the contact angle of CdS−NH_3^+ layer in the ordered (CdS−NH_3^+/PSS) films, the change in surface wettability of CdS−NH_3^+ layers of two different spin SA (CdS−NH_3^+/poly(methacrylic acid) (PMAA)) multilayer films with ordered and disordered internal structure is also investigated. The films with ordered and disordered internal structure were fabricated by the pH adjustment of PMAA. The CdS−NH_3^+ layer in both CdS−NH_3^+/PSS and CdS−NH_3^+/PMAA multilayer films with the ordered internal structure has the contact angle of about 25 ± 2° irrespective of the PSS or PMAA sublayer. As a result, the same surface wettability of PE or inorganic layers, despite different sublayers, strongly indicates that the spin SA method in optimum condition allows the top surface to be completely covered with a low level of interdigitation with a sublayer at each deposition step, and this leads to the conclusion that physical and chemical characteristics of the sublayers have no significant influence on those of the outermost layer.

Introduction

Polyelectrolyte (PE) multilayer films prepared by the dip self-assembly (SA) method have widely been utilized for the preparation of membrane,[1−5] bioactive enzyme thin films,[6−8] light-emitting diode,[9−14] particle surface modification,[15−21] and selective area patterning.[22−25] Since the introduction of the dip SA method in 1991 by Decher et al., inorganic nanoparticles as well as numerous organic species have been used to form the multilayer films through electrostatic[26−28] and hydrogen bonding interactions.[29] This conventional dip SA method is principally based on the self-diffusion process in which charged PE chains are electrostatically adsorbed onto an oppositely charged surface immersed into a PE deposition solution. Therefore, the adsorption mechanism for the dip SA multilayer films can significantly increase the level of PE interdigitation, causing the diffuse layer interface between adjacent layers.[28] Lösche et al. reported that the precision in determining the thickness of a single deuterated layer within a protonated PE/deuterated PE multilayer film is rather poor because the apparent interfacial roughness between the protonated and the deuterated strata is comparable with the deuterated layer thickness.[30] Consequently, the formed multilayer films have the disordered and intermeshed structure without clear distinction between individual layers. They also, as an alternative for overcoming this problem, suggested that the stratified layer structure between protonated and deuterated PE

* To whom all correspondence should be addressed. Fax: +82-2-873-1548. E-mail: kchar@plaza.snu.ac.kr.

(1) Rmaile, H. H.; Schlenoff, J. B. *J. Am. Chem. Soc.* **2003**, *125*, 6602.
(2) Dubas, S. T.; Farhat, T. R.; Schlenoff, J. B. *J. Am. Chem. Soc.* **2001**, *123*, 5368.
(3) Balachandra, A. M.; Dai, J.; Bruening, M. L. *Macromolecules* **2002**, *35*, 3171.
(4) Dai, J.; Balachandra, A. M.; Lee, J. I.; Bruening, M. L. *Macromolecules* **2002**, *35*, 3164.
(5) Sullivan, D. M.; Bruening, M. L. *J. Am. Chem. Soc.* **2001**, *123*, 11805.
(6) Jin, W.; Shi, X.; Caruso, F. *J. Am. Chem. Soc.* **2001**, *123*, 8121.
(7) Onda, M.; Ariga, K.; Kunitake, T. *J. Biosci. Bioeng.* **1999**, *87*, 69.
(8) Onda, M.; Lvov, Y.; Ariga, K.; Kunitake, T. *Biotechnol. Bioeng.* **1996**, *82*, 502.
(9) Ho, P. K. H.; Kim, J.-S.; Burroughs, J. H.; Becker, H.; Li, S. F. Y.; Brown, T. M.; Cacialli, F.; Friend, R. H. *Nature* **2000**, *404*, 481.
(10) Ho, P. K. H.; Granstrom, M.; Friend, R. H.; Greenham, N. C. *Adv. Mater.* **1998**, *10*, 769.
(11) Fou, A. C.; Onitsuka, O.; Ferreira, M.; Rubner, M. F.; Hsieh, B. R. *J. Appl. Phys.* **1996**, *79*, 7501.
(12) Onitsuka, O.; Fou, A. C.; Ferreira, M.; Hsieh, B. R.; Rubner, M. F. *J. Appl. Phys.* **1996**, *80*, 4067.
(13) Eckle, M.; Decher, G. *Nano Lett.* **2001**, *1*, 45.
(14) Cho, J.; Char, K.; Kim, S.-Y.; Hong, J.-D.; Lee, S. K.; Kim, D. Y. *Thin Solid Films* **2000**, *379*, 188.
(15) Caruso, F.; Caruso, R. A.; Möhwald, H. *Science* **1998**, *282*, 1111.
(16) Caruso, F.; Lichtenfeld, H.; Möhwald, H.; Giersig, M. *J. Am. Chem. Soc.* **1998**, *120*, 8523.
(17) Caruso, F.; Susha, A. S.; Giersig, M.; Möhwald, H. *Adv. Mater.* **1999**, *11*, 950.
(18) Wang, D.; Caruso, F. *Chem. Commun.* **2001**, 489.
(19) Caruso, F.; Shi, X.; Caruso, R. A.; Susha, A. *Adv. Mater.* **2001**, *13*, 740.
(20) Shi, X.; Cassagneau, T.; Caruso, F. *Langmuir* **2002**, *18*, 904.
(21) Gittins, D. I.; Susha, A. S.; Schoeler, B.; Caruso, F. *Adv. Mater.* **2002**, *14*, 508.
(22) Jiang, X.; Zheng, H.; Gourdin, S.; Hammond, P. T. *Langmuir* **2002**, *18*, 2607.
(23) Clark, S. L.; Montague, M. F.; Hammond, P. T. *Macromolecules* **1997**, *30*, 7237.
(24) Clark, S. L.; Hammond, P. T. *Adv. Mater.* **1998**, *10*, 1515.
(25) Clark, S. L.; Handy, E. S.; Rubner, M. F.; Hammond, P. T. *Adv. Mater.* **1999**, *11*, 1031.
(26) Decher, G.; Hong, J.-D.; Schmitt, J. *Macromol. Chem., Macromol. Symp.* **1991**, *46*, 321.
(27) Decher, G. *Science* **1997**, *277*, 1232.
(28) Schmitt, J.; Grünewald, T.; Decher, G.; Pershan, P. S.; Kjaer, K.; Lösche, M. *Macromolecules* **1993**, *26*, 7058.
(29) Hao. E.; Lian, T. *Chem. Mater.* **2000**, *12*, 3392. Yang, S. Y.; Rubner, M. F. *J. Am. Chem. Soc.* **2002**, *124*, 2100.
(30) Lösche, M.; Schmitt, J.; Decher, G.; Bouwman, W. G.; Kjaer, K. *Macromolecules* **1998**, *31*, 8893.

10.1021/la035476l CCC: $27.50 © 2004 American Chemical Society
Published on Web 04/17/2004

layers could be obtained by increasing the protonated PE layer thickness above the interdigitation length scale.

On the other hand, the spin self-assembly (SA) method using the spin coating, through the mechanical force operating in a direction horizontal to a substrate and the viscous force by water evaporation, provides the PE or inorganic layers with an extremely smooth surface as well as a dense surface coverage.[31−33] Accordingly, this method notably decreases the chain interdigitation and thus improves the internal structure, in that the dense coating and the surface roughness of respective layers have an important impact on the PE interdigitation between individual layers. Several years ago, Hong et al. suggested that the drying step using a spinning process after the PE adsorption using the dipping method induces a much lower level of segmental interpenetration within poly(*p*-phenylenevinylene)/poly(sodium 4-styrenesulfonate) (PSS) multilayer films than is typically observed in the dip SA multilayer films.[34]

In this regard, enhanced film qualities due to the decrease of the PE chain interpenetration between neighboring layers can provide better understanding on the surface characteristics of nanolaminated films. As an example, the surface wettability measurement, known to be quite sensitive to the chemical and physical properties of the top surface in the range of a few angstroms (Å),[35−38] is strongly influenced by the chemical structure and the chain interdigitation present in sequentially adsorbed PE layers. Yoo et al. reported that the charge density of poly(acrylic acid) (PAA), the layer thickness, and the level of layer interpenetration have a strong influence on the surface wettability of sequentially adsorbed layers of PAA and poly(allylamine hydrochloride) (PAH).[38] This implies that the surface properties of a thin layer containing a large number of chain segments coming from an underneath sublayer are much affected by the chemical characteristics of the sublayer and, on the other hand, in the case of a thick or saturated top surface, the surface properties are dominated by the chemical characteristics of the top surface layer. On the basis of these reported results, we expect that a dense outermost layer with a minimum level of interdigitation, possibly realized by the spin SA method, can exhibit similar surface wettability irrespective of the chemical nature of a sublayer and, furthermore, this kind of surface characteristics can be utilized to check on the internal structure of spin SA multilayer films. These assumptions prompt us to initiate a systematic study on the surface wettability of spin self-assembled multilayer films carrying ordered internal structure.

In the present study, we explore, on the basis of controlled PE concentration, the correlation between the surface wettability and the internal structure of the spin SA multilayer films. For this study, PAH/PSS and PAH/poly(methacrylic acid) (PMAA) multilayer films were prepared for the organic/organic systems. In addition, PAH/CdS−COO^-, CdS−NH_3^+/PSS, and CdS−NH_3^+/PMAA multilayer films are used as references for the organic/inorganic systems for which the internal structure can be quantitatively measured from X-ray reflectivity measurement. We believe that the use of two different types of multilayer systems (i.e., PE/PE and PE/inorganic multilayer films) plays an important role in understanding the correlation between the surface wettability and the internal structure of multilayer films.

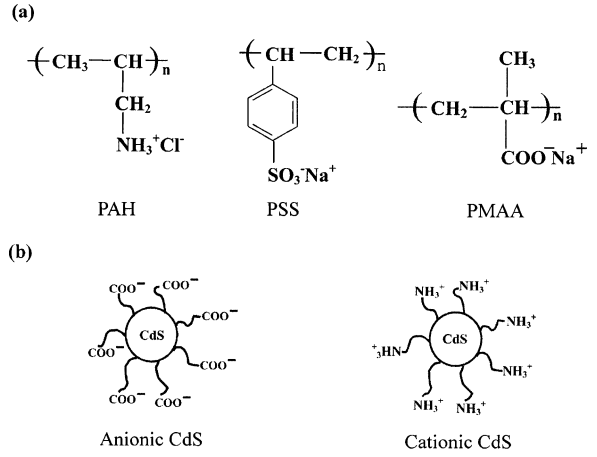

Figure 1. (a) Chemical structures of PEs and (b) cationic and anionic CdS nanoparticles used in this study.

Experimental Section

Materials. Poly(sodium 4-styrenesulfonate) (PSS; Aldrich; $M_w = 70\,000$) and poly(methacrylic acid) (PMAA; Polysciences; $M_w = 1500$) as anionic PEs and poly(allylamine hydrochloride) (PAH; Aldrich; $M_n = 50\,000-65\,000$) as a cationic PE were used. Anionic CdS nanoparticle solution was prepared using 1×10^{-3} M $Cd(ClO_4)_2$, 6×10^{-4} M mercaptoacetic acid, and 6×10^{-4} M Na_2S.[31] On the other hand, cationic CdS nanoparticle solution was obtained by treating cadmium acetate dihydrate with thioacetamide in the presence of 2-mercaptoethylamine hydrochloride.[39] The size of CdS nanoparticles was measured to be about 20 Å, as confirmed with transmission electron microscopy (TEM) and X-ray reflectivity measurements. We also found that the CdS nanoparticles were almost uniform in size. Figure 1 indicates the chemical structures of polyelectrolytes and charged CdS nanoparticles used in this study.

Build-up of Dip and Spin SA Multilayer Films. All the aqueous PE solutions except PMAA were used without pH adjustment and the addition of ionic salt in the present study. For the preparation of organic/inorganic multilayer films, CdS nanoparticles carrying carboxylic acid (−COO^-) or amine (−NH_3^+) groups on the particle surfaces were also employed.

Negatively charged silicon substrates for the deposition of positively charged PE or CdS−NH_3^+ nanoparticles were initially cleaned by ultrasonification in a hot mixture of H_2SO_4/H_2O_2 (7/3) for 3 h. They were then heated in a mixture of $H_2O/H_2O_2/NH_3$ (5/1/1) at 60 °C for 10 min and subsequently dried by N_2 gas purging. For the preparation of dip SA multilayer films, the negatively charged silicon substrates were first dipped for 20 min in the cationic PAH solution and then washed three times in water by dipping for 2 min, followed by drying with a gentle stream of nitrogen. A negatively charged PSS layer was sequentially deposited onto the positively charged substrates using the same washing and drying procedure as described above.

For the spin SA multilayer films, positively charged PE or CdS−NH_3^+ solution completely wets the total area (2 cm × 2 cm) of substrates showing the high wettability. This procedure can

(31) Cho, J.; Char, K.; Hong, J.-D.; Lee, K.-B. *Adv. Mater.* **2001**, *13*, 1076. Cho, J.; Lee, S.-H.; Kang, H.; Char, K.; Koo. J.; Seung, B. H.; Lee, K.-B. *Polymer* **2003**, *44*, 5455. Jang, H.; Kim, S.; Char, K. *Langmuir* **2003**, *19*, 3094.

(32) Chiarelli, P. A.; Johal, M. S.; Casson, J. L.; Roberts, J. B.; Robinson, J. M.; Wang, H.-L. *Adv. Mater.* **2001**, *13*, 1167. Lee, S.-S.; Hong, J.-D.; Kim, C. H.; Kim, K.; Koo, J. P.; Lee, K.-B. *Macromolecules* **2001**, *34*, 5358.

(33) Sohn, B.-H.; Kim, T.-H.; Char, K. *Langmuir* **2002**, *18*, 7770.

(34) Hong, H.; Steitz, R.; Kirstein, S.; Davidov, D. *Adv. Mater.* **1998**, *10*, 1104.

(35) Schrader, E.; Loeb, G. I. *Modern Approach to Wettability*; Plenum Press: New York, 1992.

(36) Chen, W.; McCarthy, T. J. *Macromolecules* **1997**, *30*, 78.

(37) Troughton, E. B.; Bain, C. D.; Whitesides, G. M.; Nuzzo, R. G.; Allara, D. L.; Porter, M. D. *Langmuir* **1988**, *4*, 365. Bain, C. D.; Whitesides, G. M. *Science* **1988**, *240*, 62. Liu, Y.; Wang, A.; Claus, R. O. *Appl. Phys. Lett.* **1997**, *71*, 2265. Shiratori, S. S.; Rubner, M. F. *Macromolecules* **2000**, *33*, 4213.

(38) Yoo, D.; Shiratori, S. S.; Rubner, M. F. *Macromolecules* **1998**, *31*, 4309.

(39) Chen, S. H.; Kimura, K. *Chem. Lett.* **1999**, *3*, 233.

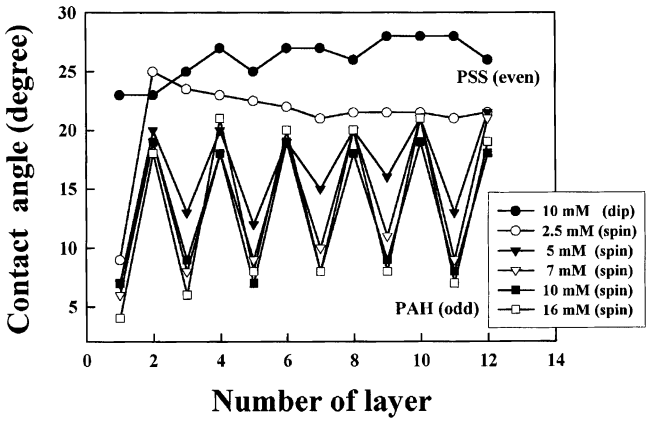

Figure 2. Water contact angles measured from PAH/PSS multilayers prepared with dip SA and spin SA methods. Odd and even numbers indicate the layers deposited with PAH and PSS, respectively.

produce a uniform film on a large area except the edge of a substrate. After the solution deposition, the substrate was rotated with a spinner at a fixed rotating speed (typically, 4000 rpm) for a short period (typically about 15 s) until a sufficiently dried film was obtained and the substrates was then thoroughly rinsed twice at a speed of 4000 rpm with plenty of deioninzed water. A negatively charged PSS layer was also sequentially deposited onto the substrate using the same procedure as mentioned above.

X-ray Reflectometry. The internal structure and film thickness of PE/inorganic multilayer films were determined by X-ray reflectivity using a Cu Kα ($\lambda = 1.54$ Å) beam from a narrow line source of a 18 kW Rigaku Ru-300 rotating anode generator. An ellipsometer (Auto EL-II) was also employed for the determination of the thickness of organic/organic multilayer films.

Measurement of Contact Angle. The contact angle of water on the self-assembled films was measured using an Advanced Surface Technology video contact angle device. To establish the relationship between internal structure and surface wettability of the multilayer films, the contact angles were measured after the deposition of each layer followed by spin washing with deionized water.

Atomic Force Measurement. The surface morphology and surface roughness of dip and spin self-assembled multilayer films were investigated using the tapping mode of atomic force measurement (AFM; Nanoscope III).

Results and Discussion

Figure 2 shows the change in water contact angles of dip and spin SA $(PAH/PSS)_n$ films when the top surface layer is alternatively changed from PAH to PSS or from PSS to PAH. Odd and even numbers represent the top surface layers of PAH and PSS, respectively. First, in the case of the dip SA film repeatedly deposited from PE solutions of 10 mM without the addition of ionic salt, all the contact angles measured after the deposition of PAH or PSS except the first two layers are within the range of 25−28° without showing the distinct periodic oscillation in contact angles. Chen and McCarthy reported that the PAH/PSS multilayer films, deposited from PE solutions of 20 mM with ionic salt added onto negatively charged poly(ethylene terephthalate) (PET) substrates, exhibit more distinct periodic oscillation in the contact angle compared with the multilayer films deposited without the addition of ionic salt when the top surface layer of PAH or PSS is alternately varied.[36] They suggested that this oscillation in the contact angles was mainly attributed to the periodical change in the surface properties of the top surface layer and, additionally, the wettability of multilayer films with a thin top layer is significantly influenced by the sublayer underneath. As a result, the disappearance of the oscillatory trend in contact angle obtained from our experimental conditions reflects that the individual layers form rather disordered layers (i.e., mixed layers) composed of interdigitated PAH and PSS segments due to the insufficient surface coverage as well as to the high surface roughness of 8 Å compared with the approximate bilayer thickness of 4 Å.[31,37]

Table 1. Thickness and Surface Roughness of Spin Self-Assembled Top Surface Layers Deposited with Different Concentrations of Polyelectrolytes

mole concn of PAH and PSS (mM)	top surface layer	thickness (Å)	RMS roughness of surface (Å)
2.5	PAH	2 ± 2	2
	PSS	5 ± 1	3
5	PAH	4 ± 3	3
	PSS	8 ± 2	4
7	PAH	5 ± 1	2
	PSS	12 ± 2	3
10	PAH	7 ± 3	3
	PSS	17 ± 4	3
16	PAH	9 ± 3	5
	PSS	21 ± 4	6

In contrast, for the spin SA multilayer films deposited from five different mole concentrations of the PE solutions, the increase in the PE concentration significantly enhances the oscillation behavior of the contact angle up to about 7 mM and then levels off at higher PE concentrations. The contact angles of both PAH and PSS top surface layers are also found to be quite low in comparison with those of the dip SA films. This result is even more intriguing when the individual thickness (measured by ellipsometry) and surface roughness (obtained by AFM) of the PAH and PSS top surface layers are taken into account, as shown in Table 1. For the spin SA films prepared with a PE concentration of 2.5 mM, it is noted that the PAH layer with 2 Å thickness and the PSS layer with 5 Å thickness, carrying a surface roughness of about 2−3 Å, do not seem to establish a well-ordered laminate structure because of the insufficient surface coverage as mentioned above. This assumption is supported by the fact that the contact angles obtained from a PE concentration of 2.5 mM indicate no periodic oscillation when the top surface layers are alternately changed. However, the relatively thick top surface layers prepared by PE concentrations above 7 mM, fully covering the layer underneath, yield distinct periodic oscillations in contact angle.

Additionally, it is noted that the top surface layers (i.e., PAH and PSS) deposited with PE concentrations of 7, 10, and 16 mM in the spin SA multilayer films demonstrate similar contact angles despite the increase in individual layer thickness. The same values in contact angle can be explained in light of physical and chemical characteristics. The formation of the top surface layers with sufficient surface coverage as well as with extremely smooth surface significantly contributes to the screening of surface effects of the sublayer by decreasing the length scale of interdigitated layers that can share the chemical properties of the top PAH or PSS layer. Sohn et al. have demonstrated that the PAH/PAA layers in the spin SA multilayer films composed of the PAH/PAA and the TiO_2 nanoparticles could strongly suppress the diffusion of probe molecules (iodide and methyl orange) through the multilayer film for a photocatalytic reaction while there is no such diffusion barrier in the dip SA films.[33] Also, we cannot exclude the possibility that the short adsorption time below 20 s as well as the strong mechanical force in a direction parallel to the substrate in the case of the spin SA method reduces the interpenetration of the PE chains.[34] It is well-known in the dip SA multilayer films that previously adsorbed PE chains are exposed to the surface in hydrated and

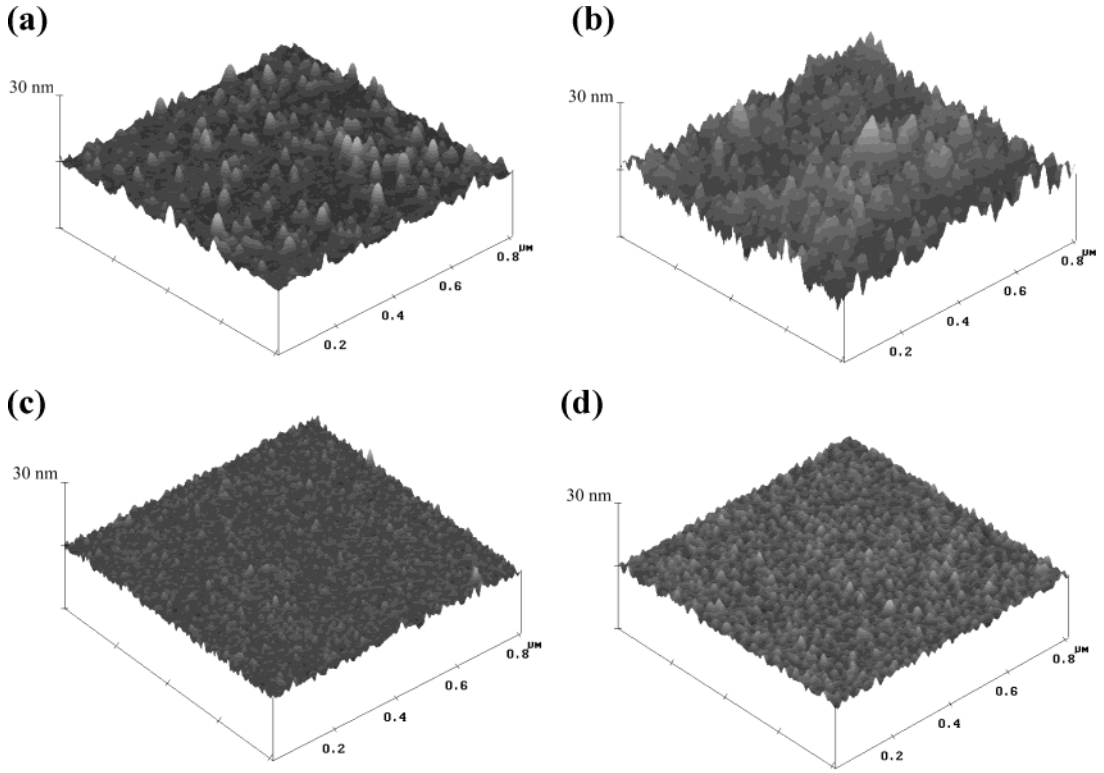

Figure 3. Tapping-mode AFM images of (a) dip SA $(PAH/CdS-COO^-)_{20}$, (b) dip SA $(CdS-NH_3^+/PSS)_{20}$, (c) spin SA $(PAH/CdS-COO^-)_{20}$, and (d) spin SA $(CdS-NH_3^+/PSS)_{20}$ multilayer films.

expanded form during the dipping in solution for a relatively long adsorption time, and thus, the preadsorbed PE is easily interpenetrated into the next adsorbing layer.[38] On the basis of these results, we strongly believe that the PE multilayer films prepared with the spin SA method can significantly reduce the level of interdigitation between adjacent layers in comparison with the dip SA films.

To confirm our hypothesis and better understand the surface characteristics of the spin SA films, we prepared spin SA $(PAH/CdS-COO^-)_{20}$ and $(CdS-NH_3^+/PSS)_{20}$ multilayer films employing PEs and inorganic CdS nanoparticles with diameters of about 2 nm and then investigated the internal structure of the multilayer films and the water contact angle of top surface layers in connection with the surface coverage. The mole concentrations of PAH, PSS, anionic $CdS-COO^-$, and cationic $CdS-NH_3^+$ solutions were adjusted to 10, 10, 0.6, and 5 mM, respectively. We point out here that all the experimental conditions for the deposition of PEs are fully consistent with those shown in Figure 2.

Figure 3 shows the AFM images of $(PAH/CdS-COO^-)_{20}$ and $(CdS-NH_3^+/PSS)_{20}$ multilayer films prepared with both the dip and the spin SA methods. In the case of the dip SA multilayer films shown in Figure 3a,b, the surface roughnesses with inorganic nanoparticle layers on top are about 18 and 25 Å despite the average bilayer thicknesses of about 6 and 7 Å, respectively. Both the relatively high surface roughnesses and the bilayer thicknesses much smaller than the average CdS nanoparticle size of 19 Å strongly suggest that the internal structure of the dip SA multilayer films, due to the insufficient surface coverage of an individual layer, is not well-ordered but rather disordered and/or mixed. As mentioned earlier, when the top surface layer is changed from a PE to an inorganic nanoparticle layer or from an inorganic nanoparticle to a PE layer, it is not difficult to assume that the surface characteristics of the top surface layer is significantly influenced by those of the sublayers. In contrast, the AFM images of the spin SA multilayer films shown in Figure 3c,d represent the extremely smooth top surface as well as the high packing density involving inorganic nanoparticles. These top surface layers show the smooth surface roughnesses of about 3 Å, and additionally, the thicknesses of PAH, $CdS-COO^-$, PSS, and $CdS-NH_3^+$ layers are estimated to be about 7, 19, 10, and 22 Å, respectively. Furthermore, as shown in Figure 4a, the spin SA $(PAH/CdS-COO^-)_{20}$ and $(CdS-NH_3^+/PSS)_{20}$ films exhibit distinct Bragg peaks at 2θ near 3.2°, indicating the well-ordered nanolaminate structure as well as the dense surface coverage of individual layers (X-ray reflectivity data of spin SA $(PAH/CdS-COO^-)_{20}$ published in our previous paper[31] is used here for detailed explanation).

On the basis of information on the internal structure and the surface roughness as well as the bilayer thickness of the PE/inorganic nanoparticle multilayer films, the change in water contact angle was also investigated when the top surface layer is varied from an inorganic to a PE layer or vice versa. It is noted that the evident oscillations in the contact angle are again caused by the well-defined internal structure as presented in Figure 4b. In particular, it is quite interesting to note that the contact angles of top surface PE layers are $6 \pm 1°$ (for PAH layers) and $19 \pm 1°$ (for PSS layers except second and fourth layers), which are fully consistent with the contact angles of the spin SA PAH/PSS films prepared with a PE concentration of 10 mM (see Figure 2). It is also reasonable to postulate that the PE chains would have more difficulty in infiltrating through a dense layer of inorganic nanoparticles than the PE layer undergoing chain reorganization and swelling during the adsorption period. Consequently, the consistency in the contact angle data evidently suggests that the surface wettability of the top surface PAH or PSS layer is not significantly affected by various parameters such as charge density and chemical structure related to

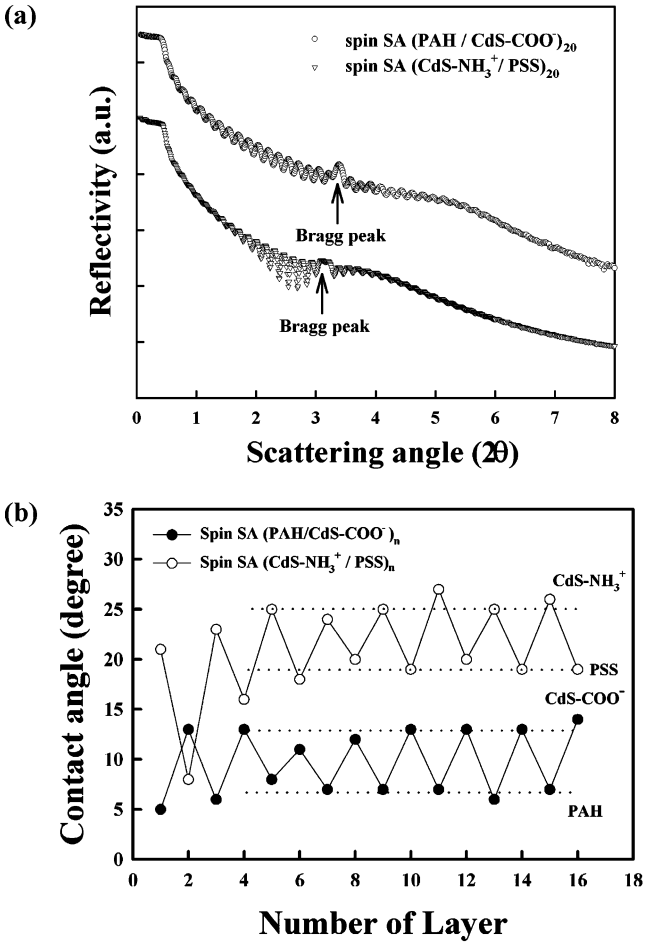

Figure 4. (a) X-ray reflectivity spectra of $(PAH/CdS-COO^-)_{20}$ and $(CdS-NH_3^+/PSS)_{20}$ multilayer films prepared with the spin SA method. (b) Water contact angles measured from $(PAH/CdS-COO^-)_n$ and $(CdS-NH_3^+/PSS)_n$ films prepared with the spin SA method. Horizontal dotted lines indicate the saturation of contact angles.

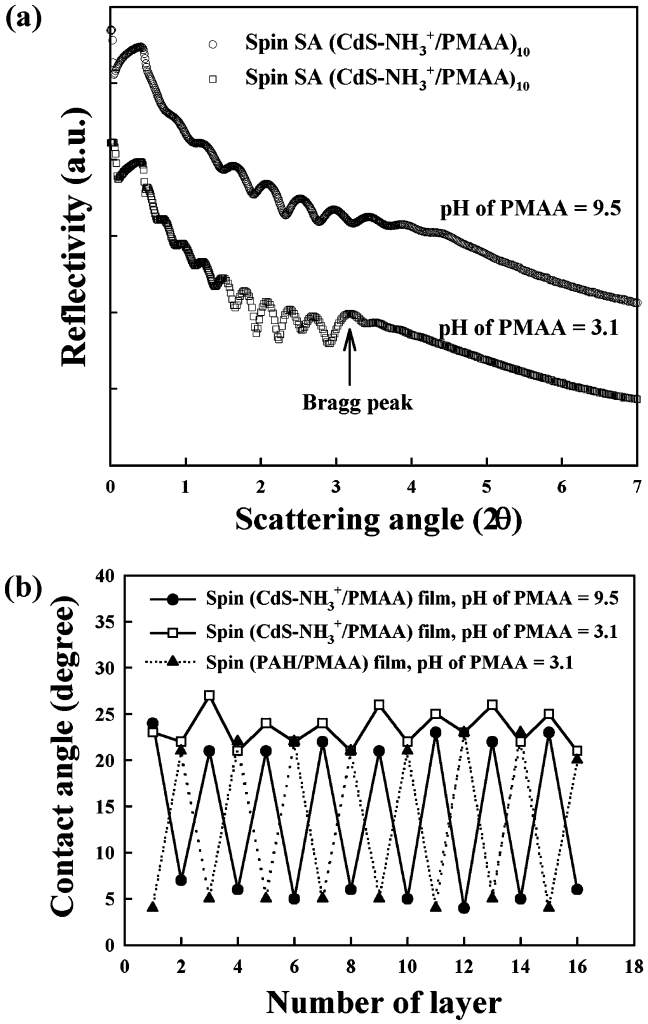

Figure 5. (a) X-ray reflectivity spectra of spin SA (cationic $CdS-NH_3^+/PMAA)_{10}$ multilayer films prepared with different pH values of PMAA. (b) Water contact angles measured from the spin SA $(CdS-NH_3^+/PMAA)_n$ films prepared with different pH values of PMAA. Odd numbers indicate the $CdS-NH_3^+$ or PAH and even numbers represent the PMAA layers. Water contact angles for the spin SA $(PAH/PMAA)_n$ films (odd numbers with PAH layer and even numbers with PMAA layer) are also shown for comparison.

the sublayer due to the enhanced surface coverage, which can be realized with the spin SA. Furthermore, it is reasonable to conclude that the internal structure of the spin SA PAH/PSS multilayer films is almost identical with that of $(PAH/CdS-COO^-)_{20}$ and $(CdS-NH_3^+/PSS)_{20}$ films.

The correlation between internal structure and contact angle is demonstrated in Figure 5. In the case of a spin SA $(CdS-NH_3^+/PMAA)_{10}$ film prepared with a PMAA solution of pH 9.5, the average bilayer thickness is 18 Å, which is smaller than the cationic CdS nanoparticle size of about 20 Å as previously mentioned. Consequently, the X-ray reflectivity curve of the spin SA $(CdS-NH_3^+/PMAA)_{10}$ film shown in the upper curve of Figure 5a does not exhibit a distinct Bragg peak. In contrast, when the pH of PMAA solution is lowered from 9.5 to 3.1, the bilayer thickness of the $(CdS-NH_3^+/PMAA)_{10}$ film increases from 18 to 28 Å and the Bragg peak clearly appears at $2\theta = 3.2°$, as shown in the lower curve of Figure 5a. The formation of a nanolaminate structure as well as the increase in bilayer thickness by pH adjustment of the PMAA solution can be explained as follows: First, the degree of ionization of PMAA carrying carboxylic acid groups is decreased with the decrease in pH, yielding a thick PMAA layer caused by the entangled chain structure.[40] Second, for the case of the spin SA method, the packing density of $CdS-NH_3^+$ nanoparticles adsorbed on the densely packed PMAA layer could also increase due to the increased surface coverage of the PE sublayer. This effect is supported by the observation that the adsorbed amount of $CdS-NH_3^+$ nanoparticles deposited from a fixed concentration significantly increases with increasing the solution concentration of PMAA from 1 to 8 mM and is then saturated at higher concentrations.

Based on these X-ray reflectivity results, the surface wettability measurement on the two different spin SA $(CdS-NH_3^+/PMAA)_n$ films showing different internal structures was also performed, as shown in Figure 5b. Water contact angles of a spin SA $(CdS-NH_3^+/PMAA)_n$ film with rather disordered internal structure (i.e., the films spin-assembled with a PMAA solution of pH 9.5) periodically vary from 21−23° (for $CdS-NH_3^+$) to 4−5° (for PMAA) when the top surface layer is switched from $CdS-NH_3^+$ to PMAA. Although these contact angles indicate distinct periodic variation by alternating the top surface layers, it should be noted that the contact angle of $CdS-NH_3^+$ is relatively low in comparison with the saturation value of $CdS-NH_3^+$ (i.e., 23−27°) shown in

(40) Mendelsohn, J. D.; Barrett, C. J.; Chan, V. V.; Pal, A. J.; Mayes, A. M.; Rubner, M. F. *Langmuir* **2000**, *16*, 5017. Yang, S. Y.; Rubner, M. F. *J. Am. Chem. Soc.* **2002**, *124*, 2100.

the well-ordered multilayer films of Figure 4b. On the other hand, in the case of the spin SA $(CdS-NH_3^+/PMAA)_n$ deposited from a PMAA solution of pH 3.1, the contact angles of the top $CdS-NH_3^+$ layer and the PMAA layer are increased to 24−27 and 21−23°, respectively. These similar contact angles of the top $CdS-NH_3^+$ layers in both spin SA $(CdS-NH_3^+/PSS)_n$ and $(CdS-NH_3^+/PMAA)_n$ films retaining the highly ordered internal structures, as shown in Figures 4b and 5b, support that the densely packed top surface layers effectively screen the chemical and physical properties of the sublayer as discussed earlier. In addition, the notable increase in the contact angle of the PMAA layer is mainly attributed to the increase of nonionized carboxylic acid groups of PMAA upon the decrease in pH of PMAA solution from pH 9.5 to 3.1.[38,40] These results were also confirmed by the preparation of spin SA $(PAH/PMAA)_n$ films with a PMAA solution of pH 3.1, as shown Figure 5b. As expected, the respective contact angles of the PAH and the PMAA top surfaces are exactly identical to the respective values shown in the spin SA $(PAH/CdS-COO^-)_{20}$ (Figure 4b) and $(CdS-NH_3^+/PMAA)_n$ (Figure 5b) films.

From a series of surface wettability measurements and internal structure analyses of the spin self-assembled PE/inorganic as well as the PE/PE multilayer films, we note that the water contact angles measured from the top surface layers are closely related to the internal structure of the multilayer films. This relationship is evident from the fact that the contact angles of a given top surface layer deposited onto sublayers of a different chemical nature yield the same values only if the individual layer of the multilayer films effectively blocks the formation of interdigitated segments between adjacent layers due to the sufficient surface coverage of each layer. Also, the results shown in the present study support the possibility that the spin SA $(PAH/PSS)_n$ multilayer films prepared with PE concentrations above about 7 mM can retain the improved internal structure in comparison with the dip SA multilayer films. Although the existence of Bragg peak and the degree of interdigitation between adjacent PE layers have not been confirmed by techniques such as neutron reflectivity, the distinct periodic variation in saturated contact angles caused by the alternate deposition of PAH and PSS layers, the relatively thick top surface layer, and the extremely low surface roughness combine to lead to the conclusion that the spin SA PE/PE multilayer films have highly ordered laminate structure within the film.

Conclusions

It is demonstrated in the present study that the surface wettability measured from the spin SA multilayer films clearly reflects their internal structure. This fact has also been supported by the supplementary results based on the measurement of both thickness and surface roughness of the top surface layers. At PE solutions with a concentration ranging from 7 to 16 mM, the distinct oscillations in water contact angle were observed with saturated values (i.e., $6 \pm 1°$ for PAH and $19 \pm 1°$ for PSS layers) when the extremely smooth top surface layer is varied from PAH to PSS or vice versa. These water contact angle values are identical to the contact angles of PE layers measured from $PAH/CdS-COO^-$ and $CdS-NH_3^+/PSS$ films verifying the distinct interfaces between PE and inorganic nanoparticle layers. Furthermore, the water contact angles for the $CdS-NH_3^+$ layers adsorbed onto different PE sublayers, as shown in the highly ordered $CdS-NH_3^+/PSS$ and $CdS-NH_3^+/PMAA$ multilayer films, also indicate the same saturated contact angles in the range of 24−27°. This consistency in the contact angles clearly suggests that the physical and chemical properties of densely packed PE or inorganic layer, which can be realized by the spin SA method, are not significantly affected by those of the sublayer. Consequently, the top surface PE layers deposited with PE concentrations yielding saturated contact angles can effectively screen the interdigitation between adjacent layers and eventually establish the improved internal structure across the film thickness.

Acknowledgment. This work was supported by the National Research Laboratory fund (Grant M1-0104-00-0191) and by the National R&D Project for Nano Science and Technology from the Ministry of Science and Technology (MOST), the Ministry of Education through the Brain Korea 21 Program at Seoul National University. X-ray reflectivity experiments performed at the Pohang Light Source (PLS) were also supported in part by MOST and POSCO.

LA035476L